

Lattice extraction of the Collins-Soper kernel using the auxiliary field representation of the Wilson line

Anthony Francis,^a C.-J. David Lin,^{a,b} Wayne Morris^{a,*} and Yong Zhao^c

^a*Institute of Physics, National Yang Ming Chiao Tung University,
1001 Ta-Hsueh Road, Hsinchu 30010, Taiwan*

^b*Centre for High Energy Physics, Chung-Yuan Christian University,
Chung-Li 32023, Taiwan*

^c*Physics Division, Argonne National Laboratory,
9700 S. Cass Avenue, Lemont, IL 60439, United States*

E-mail: waynemorris@nycu.edu.tw

The Collins-Soper (CS) kernel may be obtained through the TMD soft function by formulating the Wilson line in terms of 1-dimensional auxiliary fermion fields on the lattice. Our computation takes place in the region of the lattice that corresponds to the “spacelike” region in Minkowski space, i.e., Collins’ scheme. We explore two methods for obtaining the CS kernel. The “ratio method”; which would allow us to obtain the soft function as well as the CS kernel. And the “double ratio”; which allows us to achieve a high degree of statistical precision, but only produces the CS kernel. The matching of our result to Minkowski space is achieved through the mapping of the complex auxiliary field directional vector to the Wilson line rapidity. We present a preliminary extraction of the CS kernel using the “double ratio”, and discuss the methodology employed.

*The 42nd International Symposium on Lattice Field Theory (LATTICE2025)
2-8 November 2025
Tata Institute of Fundamental Research, Mumbai, India*

*Speaker

1. Introduction

The investigation of transverse momentum dependent (TMD) physics is a central aspect of mapping the three dimensional structure of hadrons. Well-defined TMD observables require the regularization of rapidity divergences that appear in TMD factorization formulas, and give rise to the CS kernel, which governs the rapidity evolution of TMD observables. The presence of rapidity divergences in TMD calculations, however, create a unique problem on the lattice, since rapidity has no direct analogue in Euclidean space. We propose to compute the CS kernel via the same Wilson loop operator used in the computation of the Soft function, but with directional vectors with purely imaginary time components: $\tilde{n} = (in^0, \vec{0}_\perp, n^3)$ [1, 2].

Representing the Wilson line in this way allows for a direct analytic continuation of the Euclidean soft function to its Minkowski space counterpart in the space-like regime, since the soft function is time-independent. We model the Wilson line on the lattice via the auxiliary field representation, whose equation of motion can be solved iteratively in Euclidean time. There are important issues that arise in the lattice realization of an auxiliary field propagator that will be discussed later.

There is a direct connection between this complex Wilson line direction on the Euclidean lattice and the Minkowski space rapidity defined in Collins regularization scheme [3], which we have verified to one-loop in perturbation theory. In other words, our lattice computation corresponds to the Minkowski space soft function defined with space-like directed Wilson lines.

When the Wilson line is pointing in a time-like direction, its auxiliary field representation corresponds to heavy quark effective theory (HQET). In this case, the directional vector of the Wilson line is the same as the heavy quark velocity. It was proposed in [4] to calculate the soft function using HQET, modeling the soft function as the form factor of a heavy quark pair. In this formulation, the heavy quark velocity corresponds to the time-like directed Wilson lines in Minkowski space. While our work is motivated by this proposal, it differs in two ways: our use of Euclidean directional vectors that map to space-like directions in Minkowski space, and our method for handling UV cutoff effects. Furthermore, we find that a perturbative Euclidean space computation of the soft function with directional vectors corresponding to time-like directions in Minkowski space gives a divergent integral.

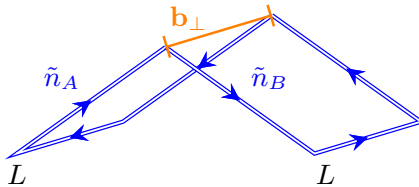


Figure 1: Butterfly loop computed in Euclidean space.

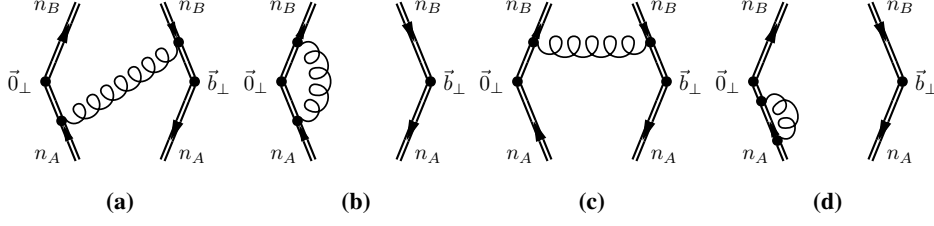


Figure 2: Diagrams contributing at one-loop to the soft function, up to mirror diagrams.

2. Theoretical considerations

We have performed a one-loop perturbative computation of the butterfly loop, Fig. 1, with infinite and finite length Wilson lines. The infinite length result establishes an equivalence between the Euclidean and Minkowski space one-loop computations. Furthermore, the finite length result can be combined into a ratio that becomes independent of Wilson line length, L , as L becomes large.

2.1 Infinite Wilson lines

To begin, we define the Euclidean space directional vectors of the Wilson lines as:

$$\tilde{n}_A \equiv (in_A^0, \vec{0}_\perp, n_A^3), \quad \tilde{n}_B \equiv (in_B^0, \vec{0}_\perp, -n_B^3). \quad (1)$$

We also define: $r_a \equiv n_A^3/n_A^0$, and $r_b \equiv n_B^3/n_B^0$ for convenience. We use dimensional regularization to handle UV divergences.

Looking at diagram (a) in Fig. 2 as an example, we perform the integration using the Schwinger parametrization and complete the square in k :

$$\begin{aligned} S_{2a}(b_\perp, \epsilon, r_a, r_b) &= g^2 C_F (\tilde{n}_A \cdot \tilde{n}_B) \int_{-\infty}^0 ds \int_{-\infty}^0 dt \int_0^\infty du \int \frac{d^d k}{(2\pi)^d} e^{-uk^2} e^{-(b_\perp + s\tilde{n}_A - t\tilde{n}_B)^2/4u} \\ &= \frac{g^2 C_F}{4\pi^{2-\epsilon}} \frac{(b_\perp^2)^\epsilon}{2\epsilon_{\text{IR}}} \frac{\Gamma(1-\epsilon)}{2} \log \left(\frac{(r_a-1)(r_b-1)}{(r_a+1)(r_b+1)} \frac{r_a r_b + 1}{r_a + r_b} \right). \end{aligned} \quad (2)$$

We obtain a finite result for diagram 2a when $|r_a|, |r_b| > 1$. This can be seen from expanding the term in the exponential of line 1 in Eq. (2):

$$(b_\perp + s\tilde{n}_A - t\tilde{n}_B)^2 = b_\perp^2 + s^2(n_A^0)^2(r_a^2 - 1) + t^2(n_B^0)^2(r_b^2 - 1) + 2stn_A^0n_B^0(r_a r_b + 1). \quad (3)$$

Equation (3) must be positive in order for the integral in Eq. (2) to converge. Because s and t can vary independently of each other, the terms on the RHS of Eq. (3) must separately be greater than zero.

The full one-loop result in Euclidean space with complex directional vectors is:

$$S(b_T, \epsilon, r_a, r_b) = 1 + \frac{\alpha_s C_F}{2\pi} \left(\frac{1}{\epsilon} + \log(\pi b_\perp^2 \mu_0^2 e^{\gamma_E}) \right) \left\{ 2 + \log \left(\frac{(r_a-1)(r_b-1)}{(r_a+1)(r_b+1)} \frac{r_a r_b + 1}{r_a + r_b} \right) \right\}. \quad (4)$$

In Minkowski space, using off light-cone directional vectors to regulate the rapidity divergence leads to two possible choices: space-like (Collins' scheme) or time-like Wilson lines:

$$\text{Time-like: } n_A = \left(1 + e^{-2y_A}, \vec{0}_\perp, 1 - e^{-2y_A}\right), \quad n_B = \left(1 + e^{2y_B}, \vec{0}_\perp, -1 + e^{2y_B}\right) \quad (5)$$

$$\text{Space-like: } n_A = \left(1 - e^{-2y_A}, \vec{0}_\perp, 1 + e^{-2y_A}\right), \quad n_B = \left(1 - e^{2y_B}, \vec{0}_\perp, -1 - e^{2y_B}\right). \quad (6)$$

Since the complex directional vectors in Euclidean space are expressed in terms of the components of their Minkowski space counterparts, we define r_a and r_b using the components of the space-like or time-like directional vectors. For the time-like case, we obtain:

$$r_a = \frac{1 - e^{-2y_A}}{1 + e^{-2y_A}}, \quad r_b = \frac{1 - e^{2y_B}}{1 + e^{2y_B}}, \quad (7)$$

where we can see that $-1 < r_a, r_b < 1$. We immediately find that this fails to satisfy the condition set by Eq. (3). As for the space-like case, we find:

$$r_a = \frac{1 + e^{-2y_A}}{1 - e^{-2y_A}}, \quad r_b = \frac{1 + e^{2y_B}}{1 - e^{2y_B}}, \quad (8)$$

which satisfies Eq. (3). The third condition, set by the last term on the RHS of Eq. (3), leads to the constraint that $n_A^0 n_B^0 (r_a r_b + 1) > 0$, which indicates that the Wilson lines must be both future pointing or both past pointing, corresponding to $e^+ e^-$ annihilation or DY type processes.

Substituting Eq. (8) into Eq. (4), we recover the Minkowski space result [5]:

$$S(b_\perp, \epsilon, y_A, y_B) = 1 + \frac{\alpha_s C_F}{2\pi} \left(\frac{1}{\epsilon} + \ln \left(\pi b_\perp^2 \mu_0^2 e^{\gamma_E} \right) \right) \left\{ 2 - 2|y_A - y_B| \frac{1 + e^{2(y_B - y_A)}}{1 - e^{2(y_B - y_A)}} \right\} + \mathcal{O}(\alpha_s^2). \quad (9)$$

Since $r_{a,b}$ directly map to the rapidities $y_{A,B}$, one can, in principle, compute the soft function for several values of $r_{a,b}$ and fit the resulting plot to obtain the intrinsic soft function, S_I in:

$$S(b_\perp, y_A, y_B, \mu) \stackrel{y_A \rightarrow +\infty}{y_B \rightarrow -\infty} = S_I(b_\perp, \mu) e^{2\gamma_q(b_\perp, \mu)(y_A - y_B)},$$

and the CS kernel:

$$\gamma_q(\mu, b_\perp) = \lim_{\substack{y_A \rightarrow +\infty \\ y_B \rightarrow -\infty}} \frac{1}{2} \frac{\partial}{\partial y_n} \log \left(\frac{S(b_\perp, y_n, y_B, \mu)}{S(b_\perp, y_A, y_n, \mu)} \right). \quad (10)$$

2.2 Finite Wilson lines

Lattice computations are constrained by their finite space-time volume, meaning that Wilson lines must have a finite length L . To account for this, we also perform a one-loop calculation for Wilson lines of finite length. One consequence of finite-length Wilson lines is the appearance of linear divergences in $1/a$, which behave like b_\perp/a and L/a . These divergences can be eliminated

by constructing the double ratio:

$$\begin{aligned}
S_{\text{double}}(b_{\perp,1}, b_{\perp,2}, a, r_1, r_2, L) &= \frac{S(b_{\perp,1}, a, r_1, r_1, L)}{S(b_{\perp,2}, a, r_1, r_1, L)} \bigg/ \frac{S(b_{\perp,1}, a, r_2, r_2, L)}{S(b_{\perp,2}, a, r_2, r_2, L)} \\
&= \exp \left[(\gamma_q(b_{\perp,1}, a) - \gamma_q(b_{\perp,2}, a)) 2(y_1 - y_2) \right] \\
&\quad + \mathcal{O} \left(\frac{b_{\perp,1}^2 - b_{\perp,2}^2}{L^2} \left(\frac{1}{r_1 - 1} - \frac{1}{r_2 - 1} \right), a^2, \frac{r_{1,2} - 1}{r_{1,2} + 1} \right),
\end{aligned} \tag{11}$$

where a is some generic regulator used for the UV divergence. The b_{\perp}/a divergences are eliminated by the ratio at two different values of r , and the L/a divergences are eliminated by the ratio at two different values of b_{\perp} .

We have determined that Eq. (11) holds to one loop in perturbation theory, using a Polyakov regulator for the UV. By computing the ratio in Eq. (11) on the lattice for sufficiently large L , we expect to obtain a time-independent observable with power-suppressed corrections of order b_{\perp}^2/L^2 , since L in the lattice formulation is proportional to Euclidean time.

A consequence of Eq. (11) is that we can only obtain the difference between two values of the CS kernel at different values of b_{\perp} on the lattice. In order to obtain the CS kernel, we must then match to the CS kernel at a perturbative value of b_{\perp} .

3. Strategy of numerical implementation

A well-known result [6, 7] is that the Wilson line can be expressed in terms of a one-dimensional auxiliary fermion field that ‘‘travels’’ along the path traced by the Wilson line:

$$P \exp \left\{ -ig \int_{s_i}^{s_f} ds n^{\mu} A_{\mu}(y(s)) \right\} = Z_{\psi}^{-1} \int \mathcal{D}\psi \mathcal{D}\bar{\psi} \psi \bar{\psi} \exp \left\{ i \int_{s_i}^{s_f} ds \bar{\psi} in \cdot \partial \psi - g_0 \bar{\psi} n \cdot A \psi \right\}, \tag{12}$$

whose propagator, $H_n(x - y)$, satisfies the Green function equation:

$$in \cdot D H_n(x - y) = i \delta^{(4)}(x - y), \tag{13}$$

where $D = \partial + ig_0 A$ is the covariant derivative. The Euclidean space counterpart of Eq. (13) is defined with a directional vector with a purely imaginary time component, which can be written as $\tilde{n} = (in^0, \vec{n})$ in terms of the Minkowski space vector components. After applying a Wick rotation, the Euclidean space equation becomes:

$$i\tilde{n} \cdot D_E H_{\tilde{n}}(x_E - y_E) = \delta^{(4)}(x_E - y_E). \tag{14}$$

As discussed in [8, 9], meaningful solutions to Eq. (14) can only be obtained with a UV cutoff. Hence, using the lattice spacing as our regulator, we can construct a discretized version of this propagator. The central idea is to express the soft function in terms of lattice-regulated auxiliary field propagators, $H_{\tilde{n}}$. The soft function can be shown to possess a well-defined continuum limit.

Based on a one-loop analysis we expect the butterfly loop to behave as:

$$S_{\text{bfly}} = S(b_{\perp}, a, r_a, r_b, \tau) \xrightarrow{\tau \rightarrow \infty} e^{2\pi\tau(r_a+r_b)/a} / \tau^4 \quad (15)$$

in the large τ limit, where τ is now the Euclidean time. Noticing that the term in Eq. (15) is independent of b_{\perp} , we can construct the single ratio:

$$R_{\text{single}}(b_{\perp,1}, b_{\perp,2}, a, r_a, r_b, \tau) = \frac{S(b_{\perp,1}, a, r_a, r_b, \tau)}{S(b_{\perp,2}, a, r_a, r_b, \tau)}. \quad (16)$$

Based on our perturbative work, we expect the RHS of Eq. (15) to be an overall multiplicative factor in the large τ region; therefore, R_{single} will not suffer from the cutoff effects introduced by the Euclidean auxiliary propagator.

From here, we construct the double ratio introduced in Eq. (11) in order to remove linear divergences. The double ratio should also handle the operator renormalization, since the soft function is multiplicatively renormalizable.

We use the same method employed in [10] to solve the auxiliary field propagator on the lattice, leading to improved stability relative to the simpler method in [11, 12]. Our implementation of [10] corresponds to the infinite mass limit.

3.1 Rapidity renormalization

Lattice regularization breaks the $O(4)$ rotation symmetry in Euclidean space, leading to the need of renormalisation for the directional vectors in Eq. (1), or equivalently r_a and r_b [9]. We do not have a method to directly determine the renormalized values of r_a, r_b , but we may infer the renormalized rapidity through the relation:

$$2(y_1^{\text{ren}}(a) - y_2^{\text{ren}}(a)) = \frac{\log\left(S_{\text{double}}\left(b_{\perp,1}^{\text{pert}}, b_{\perp,2}^{\text{pert}}, r_1, r_2, a\right)\right)}{\gamma_q\left(b_{\perp,1}^{\text{pert}}, \mu\right) - \gamma_q\left(b_{\perp,2}^{\text{pert}}, \mu\right)} + \text{p.s.c.}, \quad (17)$$

where S_{double} is given in Eq. (11), y^{ren} is the renormalized rapidity, and the denominator on the RHS has two values of γ_q in the perturbative region. Also, p.s.c. refers to power suppressed corrections of the type in Eq. (11). Here, we assume the renormalization scale $\mu \sim 1/a$, such that the continuum matching is trivial. In any case, we can take advantage of the fact that the difference between two values of the CS kernel is a renormalization group invariant quantity.

Using the renormalized rapidity, we can then write down a formula for the CS kernel at any value of b_{\perp} :

$$\gamma_q(b_{\perp}, \mu) = \gamma_q\left(b_{\perp,2}^{\text{pert}}, \mu\right) + \frac{\log\left(S_{\text{double}}\left(b_{\perp}, b_{\perp,2}^{\text{pert}}, r_1, r_2, a\right)\right)}{2(y_1^{\text{ren}}(a) - y_2^{\text{ren}}(a))} + \text{p.s.c.} \quad (18)$$

4. Numerical results and discussion

For the lattice computation we used the quenched configurations given in Table 1 [13]. From Fig. 3, we find that the behavior of R_{single} is consistent with our expectations from our one-loop

$L^3 \times T$	$24^3 \times 48$	$32^3 \times 64$	$40^3 \times 80$	$48^3 \times 96$
a (fm)	0.081	0.060	0.048	0.041
N_{config}	400	400	250	341

Table 1: Quenched configurations used for computation, with lattice spacing, a , and number of configurations, N_{config} .

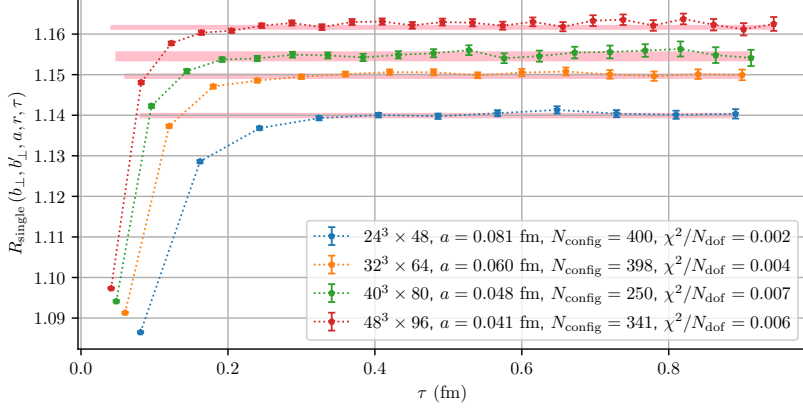


Figure 3: Single ratio plot with $b_{\perp} = 4a$, $b'_{\perp} = 3a$, and $r = 1.001$

analysis; namely, the plateau in Euclidean time suggests that UV cutoff effects are cancelled as predicted by Eqs. (15) and (16). We can then perform a constant fit of the plateau to obtain R_{single} .

Because our procedure requires that we match to perturbative values of the CS kernel, we need to ensure that we have enough lattice data in the perturbative region. For our perturbative window we choose $3a \leq b_{\perp} \leq 0.2$ fm. The lower bound was chosen to avoid discretization errors from the lattice computation, while the upper bound was chosen to reduce uncertainty in the perturbative CS kernel. Due to these restrictions, we omit the $24^3 \times 48$ and $32^3 \times 64$ lattices from the subsequent steps in our analysis procedure.

Following the procedure laid out in Sec. 3.1, we obtain the result given in Fig. 4 for several values of b_{\perp} within the perturbative window. We interpret the different results for the CS kernel at different values of b_{pert} as a systematic uncertainty related to the use of fixed-order ($N^3\text{LO}$) perturbative results.

In order to account for the systematic uncertainty, we perform our routine for extracting the CS kernel for all possible values of b_{pert} within the matching window. Additionally, we vary the renormalization scale of the $\overline{\text{MS}}$ -scheme CS kernel used in the extraction by 10% around a central value of 2 GeV. Performing an average over these results gives us a conservative estimate of the systematic error associated with our method, as exhibited in Fig. 5.

5. Conclusions

We have demonstrated to one-loop in perturbation theory that the auxiliary field method for extracting the CS kernel from a lattice computation has a strong theoretical motivation. Particularly,

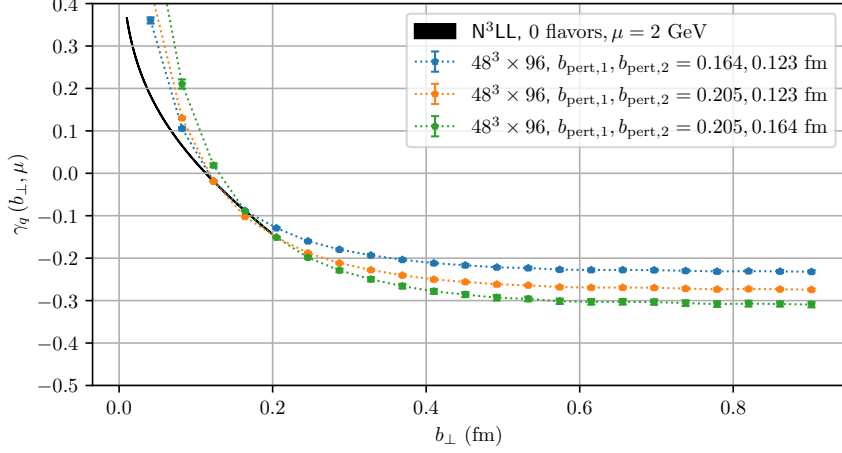


Figure 4: CS kernel extracted on the ensemble with $a = 0.041$ fm at different $b_{\text{pert},1}, b_{\text{pert},2}$ within matching window.

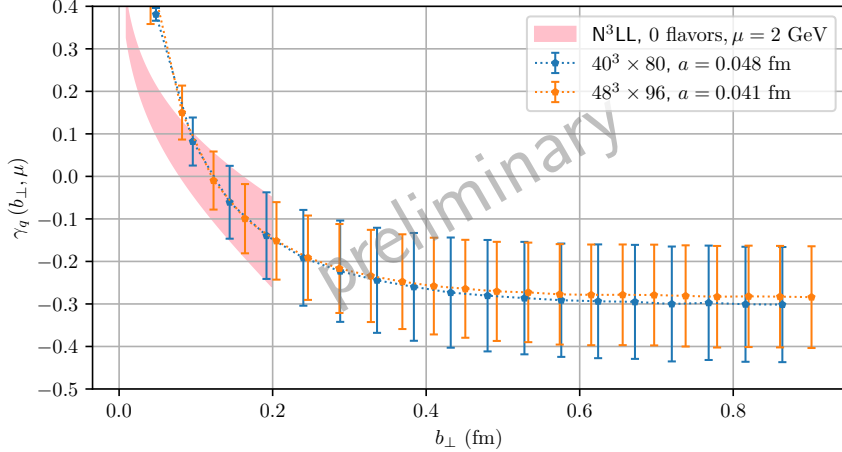


Figure 5: The CS kernel extracted by our method, with a conservative estimate of systematic error from matching points within fit window and variation of UV scale

there is a direct mapping between the Euclidean computation of the butterfly loop and the Minkowski space result at large lattice time. The double ratio method for computing the CS kernel difference, $\gamma_q(b_\perp, \mu) - \gamma_q(b'_\perp, \mu)$, allows us to obtain an high degree of statistical precision. The uncertainty in our result is dominated by systematic effects, primarily related to the necessary perturbative matching in our procedure.

We are currently processing data from $64^3 \times 128$ quenched configurations at lattice spacing $a = 0.03$ fm, which will allow us more control over the perturbative window. We are also working on a more robust analysis procedure of our data to give a better estimate of the systematic uncertainties.

Acknowledgments

We acknowledge Yizhuang Liu for helpful discussions. AF is supported by the National Science and Technology Council (NSTC) of Taiwan under grant 113-2112-M-A49-018-MY3. CJDL and WM are supported by the Taiwanese NSTC through grants 112-2112-M-A49-021-MY3, 112-2811-M-A49-517-MY2 and 114-2123-M-A49-001-SVP. The work of YZ is supported by the U.S. Department of Energy, Office of Science, Office of Nuclear Physics through Contract No. DE-AC02-06CH11357 and the Early Career Award through Contract No. DE-SCL0000017.

References

- [1] A. Francis, I. Kanamori, C.J.D. Lin, W. Morris and Y. Zhao, *The lattice extraction of the TMD soft function using the auxiliary field representation of the Wilson line*, in *40th International Symposium on Lattice Field Theory*, 12, 2023 [[2312.04315](#)].
- [2] A. Francis, I. Kanamori, C.J.D. Lin, W. Morris and Y. Zhao, *Measurement of the TMD soft function on the lattice using the auxiliary field representation of the Wilson line*, *PoS LATTICE2024* (2025) 303 [[2412.12645](#)].
- [3] J. Collins, *Foundations of Perturbative QCD*, vol. 32, Cambridge University Press (2011), [10.1017/9781009401845](#).
- [4] X. Ji, Y. Liu and Y.-S. Liu, *TMD soft function from large-momentum effective theory*, *Nucl. Phys. B* **955** (2020) 115054 [[1910.11415](#)].
- [5] M.A. Ebert, I.W. Stewart and Y. Zhao, *Towards Quasi-Transverse Momentum Dependent PDFs Computable on the Lattice*, *JHEP* **09** (2019) 037 [[1901.03685](#)].
- [6] J.-L. Gervais and A. Neveu, *The Slope of the Leading Regge Trajectory in Quantum Chromodynamics*, *Nucl. Phys. B* **163** (1980) 189.
- [7] I.Y. Arefeva, *QUANTUM CONTOUR FIELD EQUATIONS*, *Phys. Lett. B* **93** (1980) 347.
- [8] U. Aglietti, M. Crisafulli and M. Masetti, *Problems with the Euclidean formulation of heavy quark effective theories*, *Phys. Lett. B* **294** (1992) 281.
- [9] U. Aglietti, *Consistency and lattice renormalization of the effective theory for heavy quarks*, *Nucl. Phys. B* **421** (1994) 191 [[hep-ph/9304274](#)].
- [10] R.R. Horgan et al., *Moving NRQCD for heavy-to-light form factors on the lattice*, 2009. [10.1103/PhysRevD.80.074505](#).
- [11] J.E. Mandula and M.C. Ogilvie, *A Lattice implementation of the Isgur-Wise limit*, *Phys. Rev. D* **45** (1992) 2183.
- [12] J.E. Mandula and M.C. Ogilvie, *A Lattice implementation of the Isgur-Wise limit*, *Nucl. Phys. B Proc. Suppl.* **26** (1992) 459.
- [13] W. Detmold and M.G. Endres, *Scaling properties of multiscale equilibration*, *Phys. Rev. D* **97** (2018) 074507 [[1801.06132](#)].